blood®
Regular Article

MYELOID NEOPLASIA

Mutant calreticulin knockin mice develop thrombocytosis and myelofibrosis without a stem cell self-renewal advantage

Juan Li,[1,2,*] Daniel Prins,[1,2,*] Hyun Jung Park,[1,2] Jacob Grinfeld,[1-3] Carlos Gonzalez-Arias,[1-3] Stephen Loughran,[1,2] Oliver M. Dovey,[4] Thorsten Klampfl,[1,2] Cavan Bennett,[2,5] Tina L. Hamilton,[1,2] Dean C. Pask,[1,2] Rachel Sneade,[1,2] Matthew Williams,[1,2] Juliet Aungier,[1,2] Cedric Ghevaert,[2,5] George S. Vassiliou,[3,4] David G. Kent,[1,2] and Anthony R. Green[1-3]

[1]Cambridge Institute for Medical Research and Wellcome Trust/Medical Research Council Stem Cell Institute and [2]Department of Haematology, University of Cambridge, Cambridge, United Kingdom; [3]Department of Haematology, Addenbrooke's Hospital, Cambridge, United Kingdom; [4]Wellcome Trust Sanger Institute, Cambridge, United Kingdom; and [5]National Health Service Blood and Transplant, Cambridge, United Kingdom

KEY POINTS

- **Mutant CALR drives ET and MF in knockin mice.**
- **Mutant CALR expression results in expansion of phenotypic HSCs without a self-renewal advantage.**

Somatic mutations in the endoplasmic reticulum chaperone calreticulin (CALR) are detected in approximately 40% of patients with essential thrombocythemia (ET) and primary myelofibrosis (PMF). Multiple different mutations have been reported, but all result in a +1-bp frameshift and generate a novel protein C terminus. In this study, we generated a conditional mouse knockin model of the most common CALR mutation, a 52-bp deletion. The mutant novel human C-terminal sequence is integrated into the otherwise intact mouse CALR gene and results in mutant CALR expression under the control of the endogenous mouse locus. CALR$^{del/+}$ mice develop a transplantable ET-like disease with marked thrombocytosis, which is associated with increased and morphologically abnormal megakaryocytes and increased numbers of phenotypically defined hematopoietic stem cells (HSCs). Homozygous CALR$^{del/del}$ mice developed extreme thrombocytosis accompanied by features of MF, including leukocytosis, reduced hematocrit, splenomegaly, and increased bone marrow reticulin. CALR$^{del/+}$ HSCs were more proliferative in vitro, but neither CALR$^{del/+}$ nor CALR$^{del/del}$ displayed a competitive transplantation advantage in primary or secondary recipient mice. These results demonstrate the consequences of heterozygous and homozygous CALR mutations and provide a powerful model for dissecting the pathogenesis of CALR-mutant ET and PMF. (*Blood*. 2018; 131(6):649-661)

Introduction

The myeloproliferative neoplasms (MPNs) are chronic hematologic malignancies that arise in the hematopoietic stem cell (HSC) compartment and share a variable propensity to transform to acute myeloid leukemia.[1-3] The BCR-ABL–negative classic MPNs are described as falling into 3 categories: polycythemia vera (PV), essential thrombocythemia (ET), and primary myelofibrosis (PMF). PV and ET are chronic phase disorders with a relatively benign prognosis; major complications include thrombosis and myelofibrotic transformation. PMF is less common and is a more advanced disease. It closely resembles myelofibrotic transformation of PV and ET, and in many cases, it is likely to present in an accelerated phase of an undiagnosed preexisting ET.[4,5]

Most patients with 1 of the 3 classical MPNs harbor phenotypic driver mutations that affect cytokine signaling through JAK family kinases.[6] The most common lesion is an acquired JAK2^{V617F} mutation.[7-10] With the subsequent discovery of JAK2 exon 12 mutations, it is now clear that the vast majority of PV patients harbor a gain-of-function mutation in JAK2.[11] In ET and PMF, only 50% of patients carry a JAK2 mutation. Of the JAK2 nonmutated patients, approximately 5% to 10% carry a gain-of-function mutation in the thrombopoietin (THPO) receptor (MPL),[12] and a further 70% to 84% possess mutations in CALR, which encodes an endoplasmic reticulum chaperone.[6,13]

Although several different CALR mutations have been described,[2,6,13] all are deletions or insertions within exon 9 that result in a +1-bp frameshift and thereby generate a protein with a novel C terminus. Recent structure and/or function studies have elegantly shown that mutant CALR interacts with the extracellular domain of THPO receptor to activate downstream signaling and that the novel C terminus is essential for this process.[14-16] Retroviral studies[14,17] and transgenic studies[18] (in which mutant CALR complementary DNA [cDNA] was driven by the H-2K^{b} promoter and Moloney murine leukemia virus long terminal repeat) have shown that mutant CALR can generate a myeloproliferative phenotype in mice. However, the pathogenetic consequences of expressing mutant CALR in an appropriate cell type–specific manner and at physiological levels are unknown. Here, we describe the generation of knockin mice that express the most common form of mutant CALR (52-bp deletion) under the control of the mouse CALR locus.

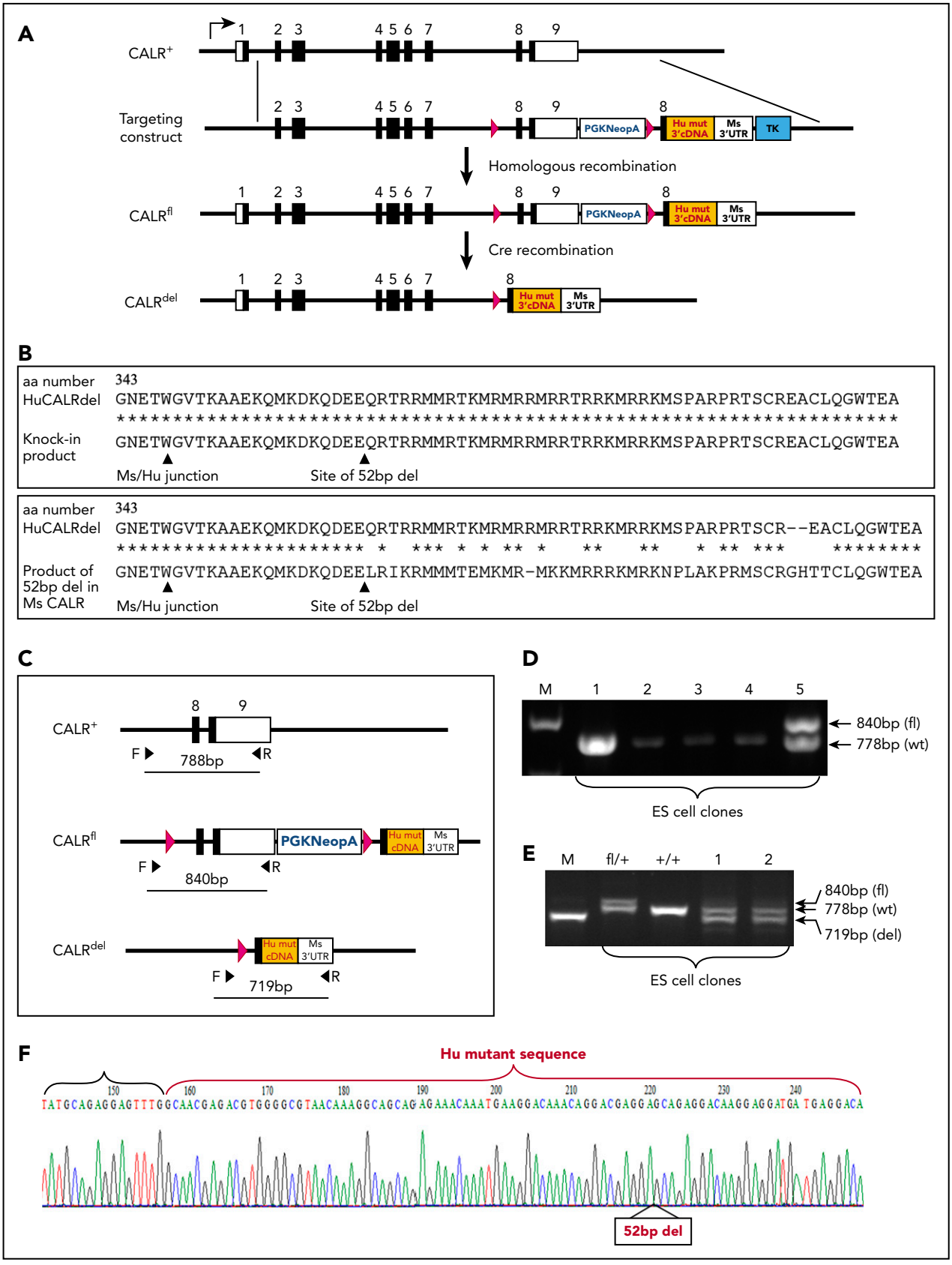

Figure 1. Generation of a conditional humanized mutant CALR knockin mouse model. (A) Diagrams showing the endogenous mouse (Ms) CALR gene locus (CALR^{+}), the targeting construct, the targeted conditional knockin allele (CALR^{fl}), and the recombined allele (CALR^{del}) after Cre recombination to remove the PGKNeopAstop cassette. The recombined allele is designed to carry the mouse CALR genomic region, including mouse exons 1 to 7 followed by the 5′ part of mouse exon 8 fused to the 3′ part of the human (Hu) mutant (mut) CALR cDNA sequence (orange). LoxP sites are indicated by red arrows. (B) Amino acid alignment of WT and mutant CALR proteins. There is a 94% identity between the

Materials and methods

Generation of hematopoietic-specific conditional knockin mice for mutant CALR

A 9.3-kb region spanning exons 2 to 9 of mouse CALR (corresponding to nucleotides 16143-25460 in the reverse complementary sequence of the mouse BAC clone RP24-341A18 [accession No. AC155163]) was manipulated to include the targeting cassettes. A LoxP site was inserted into nucleotide position 19478 of the 5′ homology arm (nucleotides 16143-20881), which was followed downstream by a PGKNeo-poly(A) minigene and another LoxP site. The 3′ homology arm (20141-25460) is preceded by sequence 19499-10782, including part of the mouse intron 7 and of exon 8, which was fused at the BsmBI site with the mutant human CALR cDNA sequence (corresponding to nucleotides 1095-1350 [accession No. BC020493]). A thymidine kinase (TK) minigene located downstream of the 3′ homology arm was also included in the targeting vector. The targeting plasmid DNA linearized with *NotI* was used for gene targeting in embryonic stem (ES) cells (JM8 in C57BL/6N background), and ES clones resistant to G418 and FIAU were selected. ES clones with correctly targeted alleles (designated $CALR^{fl/+}$) were injected into albino C57BL/6 blastocysts, and chimeras were bred with C57BL/6 mice to generate germ line heterozygous $CALR^{fl/+}$ mice. All mice were kept in specific-pathogen-free conditions, and all procedures were performed according to United Kingdom Home Office regulations.

Bone marrow transplantation assays

For transplantation assays, $Kit^{W41/W41}$ (CD45.1) recipients were irradiated with 400 cGy and C57BL/6 (CD45.1) recipients were irradiated with 2 × 550 cGy. The $Kit^{W41/W41}$ strain is derived from C57BL/6, which requires only a sublethal dose of radiation and is more permissive for donor cell engraftment because the endogenous HSCs are >10-fold less functional. For noncompetitive transplantation assays, 2×10^6 nucleated bone marrow (BM) cells were injected into recipient mice. Peripheral blood was obtained every 4 weeks at which time full blood counts were performed, and donor cell repopulation was examined by flow cytometric analysis using CD45.1 and CD45.2 antibodies (BD Biosciences). For competitive repopulation assays, 1×10^6 nucleated competitor BM cells (a 1:1 ratio) were obtained from CD45.1/CD45.2 F_1 mice and injected into recipient mice. For secondary BM transplantation, 5×10^6 nucleated BM cells from primary recipients were injected into recipient mice. In all cases, peripheral blood was obtained and analyzed by flow cytometry for donor contribution to myeloid (Ly6g and Mac1) and lymphoid (B220 and CD3e) cells.

Single HSC in vitro cultures

In vitro culture of single E-SLAM HSCs was performed as previously described.[19,20] E-SLAM HSCs were sorted into round-bottom 96-well plates, preloaded with 50 μL serum-free Stemspan medium (STEMCELL Technologies). A further 50 μL of medium was subsequently added to each well to a final concentration of 10% fetal calf serum, 1% penicillin/streptomycin, 1% L-glutamine, 300 ng/mL stem cell factor (STEMCELL Technologies), 20 ng/mL interleukin-11 (STEMCELL Technologies), and 0.1 mM β-mercaptoethanol. For cell division kinetics, the number of cells in each well was counted manually every day for up to 4 days in culture. To evaluate the number and proportion of mature cell types produced by single E-SLAM HSCs in vitro, after 7 days in culture, clonal cells were stained with antibodies for lineage markers (CD3, Ly6G/Ly6C, CD11b, CD45R/B220, Ter119), Sca-1 BV605 and c-Kit APC/Cy7 to assess the frequencies of LSK ($Lin^-Sca\text{-}1^+c\text{-}Kit^+$) and lineage-positive cells. Lineage output of single-cell cultures was also analyzed after 14 days by using flow cytometry with antibodies for Mac1 allophycocyanin, CD41 phycoerythrin, and CD71 fluorescein isothiocyanate.

Statistics

The statistical differences between control and mutant mice were assessed by using a two-tailed unpaired Student *t* test, unless otherwise indicated.

Results

Generation of conditional mutant CALR knockin mice

To study the role of CALR mutations in the pathogenesis of MPNs, we generated a conditional knockin allele in murine ES cells by using homologous recombination for the most common CALR mutation (52-bp deletion) (Figure 1A). Species-specific differences in codon preferences meant that simply generating an analogous 52-bp deletion within the mouse sequence would generate a novel C terminus substantially different from that seen in ET patients (Figure 1B). We therefore adopted a strategy in which the targeted allele ($CALR^{fl}$) contained a LoxP site in intron 7 and a PGKNeo-polyA LoxP cassette followed by a mouse exon 8 fused with mutant human CALR 3′ cDNA sequence downstream of exon 9 (Figure 1A; supplemental Figure 1A, available on the *Blood* Web site). This approach allowed the generation of a conditional allele that expresses a mutant CALR protein with a carboxy-terminal amino acid sequence identical to that found in MPN patients while keeping the mouse sequence otherwise intact (Figure 1B). The targeted allele ($CALR^{fl}$) is predicted to express wild-type (WT) mouse CALR and can be induced to express humanized mutant CALR under the control of murine CALR regulatory elements upon removal of the floxed mouse CALR exons and PGKNeo-polyA by Cre-mediated recombination. Correctly targeted ES clones were characterized by genomic polymerase chain reaction (PCR) (Figure 1C-D; supplemental Figure 1B). Targeted ES clones were expanded and then subjected to transient Cre expression by using a PGK-Cre plasmid. Genomic PCR confirmed the recombination of the allele (Figure 1E). Reverse

Figure 1 (continued) entire amino acid sequences of human and mouse proteins. (Top panel) Alignments show amino acid 343 to the C terminus of human mutant CALR and the designed humanized mutant CALR knockin product. (Bottom panel) The predicted product if the corresponding 52-bp region is deleted in the mouse CALR gene. Alignment was performed by using an online program available at www.expasy.org. Sites of the mouse/human junction and the 52-bp deletion are indicated. (C) Diagram showing location of the primers for PCR genotyping. F and R indicate forward and reverse primers. (D) Characterization of ES cell targeting. PCR performed on genomic DNA from ES clones (lanes 1-5) using primers F and R shown in (C). The ES clone in lane 5 is correctly targeted. (E) Characterization of Cre/LoxP-mediated recombination of targeted ES cells. PCR was performed on genomic DNA from ES cells upon Cre recombinase expression by using primers F and R as shown in panel C. fl/+, targeted ES clone; +/+, WT ES clones; lanes 1 and 2, Cre recombined ES clones. (F) Sequencing traces of RT-PCR product showing correct humanized mutant CALR expression with the 52-bp deletion indicated (52bp del). RT-PCR was performed on total RNA from an ES clone that was Cre recombined, and the PCR product was cloned and sequenced. M, DNA marker; UTR, untranslated region.

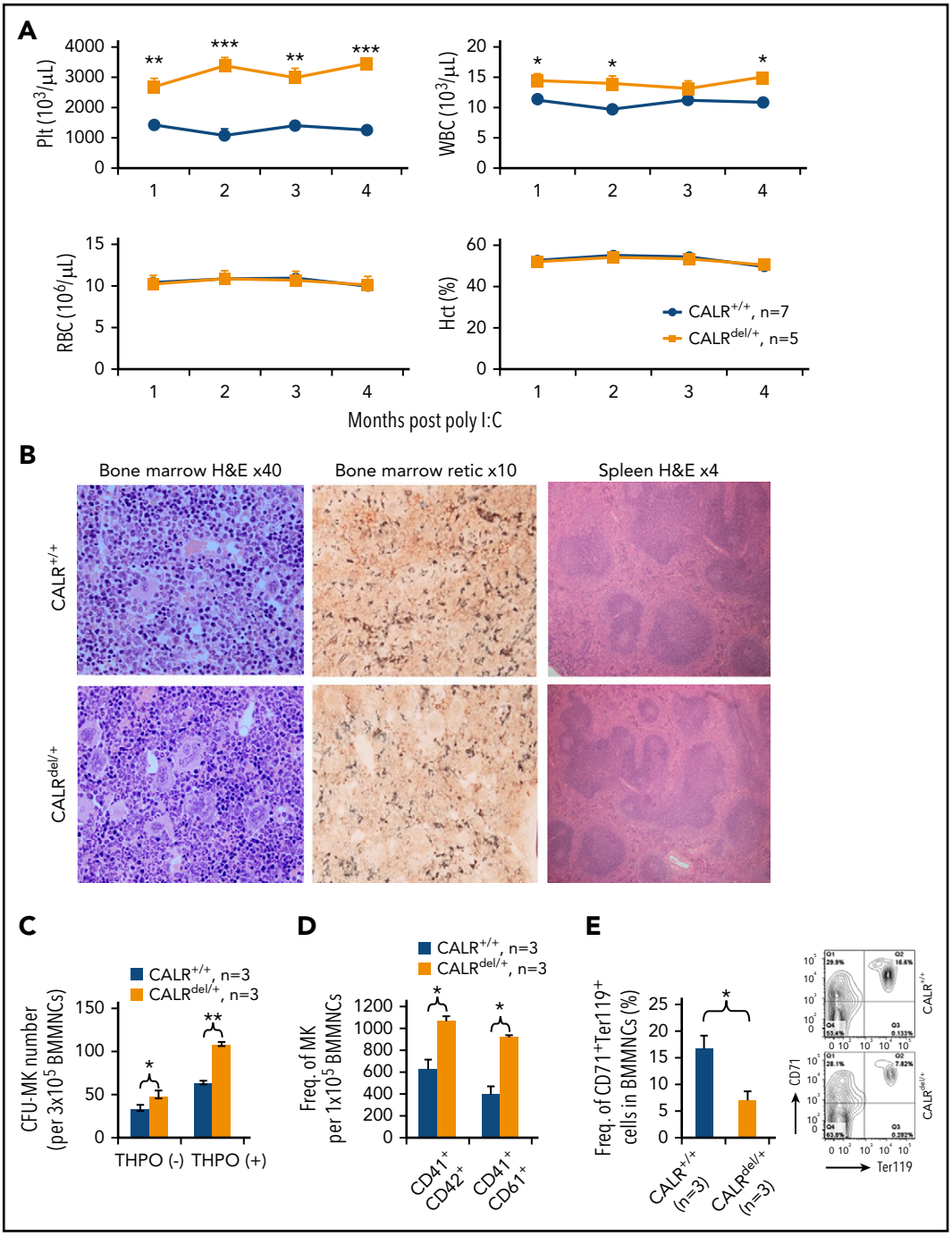

Figure 2. CALR$^{del/+}$ mice develop a myeloproliferative disease. (A) Time course of blood parameters of CALR$^{del/+}$ and control mice showing significantly increased platelets (Plt) and normal hematocrit and hemoglobin. A mildly elevated white blood cell (WBC) count is shown and is seen only in some cohorts. The CALR$^{del/+}$ mice were CALR$^{fl/+}$ Mx1Cre^{+}, and the littermate control mice CALR$^{+/+}$ were CALR$^{fl/+}$ Mx1Cre^{-} or CALR$^{+/+}$ Mx1Cre^{+}. (B) Histologic analysis showing megakaryocytic hyperplasia with increased clustering and hyperlobated nuclei without fibrosis. (Left panel) Hematoxylin and eosin (H&E) staining performed on BM from mice at 3 to 4 months after poly I:C injection. (Middle panel) BM staining for reticulin (retic) showing no fibrosis. (Right panel) H&E staining of spleen showing normal splenic architecture. (C) CALR$^{del/+}$ mice show increased megakaryocyte colonies. Bar graphs showing significantly increased number of colony-forming unit–megakaryocyte (CFU-MK) colonies in BM. CFU-MK assay was performed in media with or without THPO. (D) CALR$^{del/+}$ mice show increased megakaryocytes. Flow cytometry was performed to assess the frequency (Freq) of BM megakaryocytes (MKs) (CD41^{+}CD42^{+} or CD41^{+}CD61^{+}). (E) CALR$^{del/+}$ mice show reduced erythroblasts in BM. Flow cytometry was performed to assess the frequency of erythroblasts (CD71^{+}Ter119^{+}). Means ± standard error of the means (SEMs) are shown. *P < .05; **P < .01; ***P < .001. MNC, mononuclear cell; RBC, red blood cell.

transcription PCR (RT-PCR) was performed on total RNA from ES cells after Cre recombination, and the PCR product was cloned and sequenced to demonstrate expression of CALR messenger RNA with the 52-bp deletion (Figure 1F; supplemental Figure 1C). Correctly targeted ES cells were then injected into C57BL/6 albino blastocysts to produce chimeras. The resulting chimeric mice were bred to C57BL/6 mice to generate germ line transmission (ie, CALR$^{fl/+}$ mice). Quantitative RT-PCR

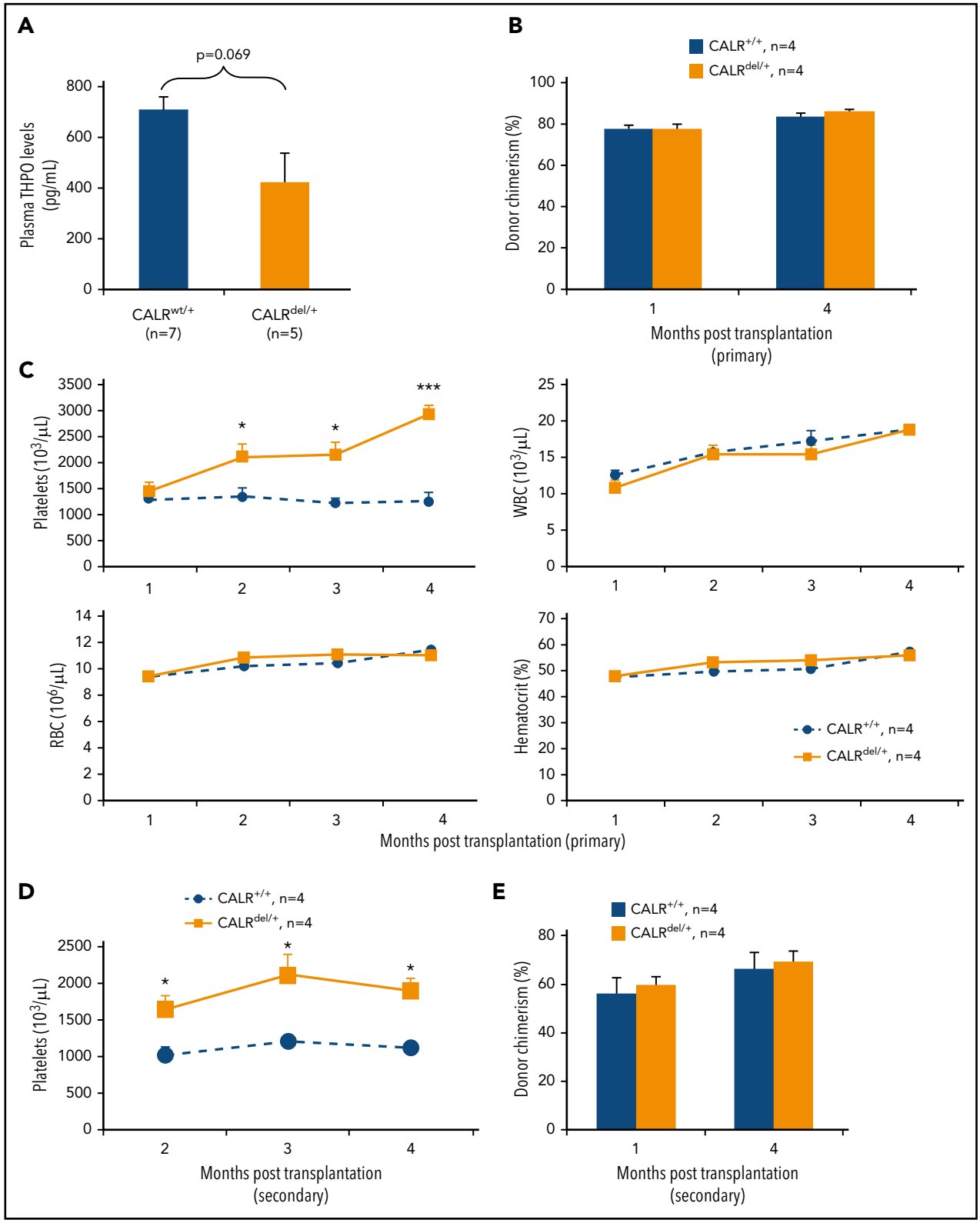

Figure 3. Thrombocytosis in CALR$^{del/+}$ mice is transplantable. (A) Plasma THPO level is not significantly altered in CALR$^{del/+}$ mice. (B) Donor chimerism is comparable in the primary noncompetitive BM transplants. BM cells from CALR$^{del/+}$ or control mice (2×10^6 per recipient) were transplanted into irradiated (2×550 cGy) CD45.1 C57BL/6 recipients. Donor chimerism in peripheral blood was analyzed by using flow cytometry with CD45.1 and CD45.2 antibodies and was derived as a percentage of CD45.2$^+$ cells in whole nucleated blood. (C) Time course of blood counts showing significantly increased platelet counts in the recipients of CALR$^{del/+}$ BM. (D) Time course of blood counts showing significantly increased platelet counts in the secondary transplant recipients of CALR$^{del/+}$ BM. BM cells from the primary recipients of CALR$^{del/+}$ or control BM (5×10^6 cells per recipient) were transplanted into irradiated (1×400 cGy) *Kit*$^{W41/W41}$ (CD45.1) recipients. (E) Donor chimerism was comparable in the secondary noncompetitive BM transplants. Donor chimerism in peripheral blood was analyzed by using flow cytometry as above. Data are shown as mean ± SEM. *$P < .05$; ***$P < .001$.

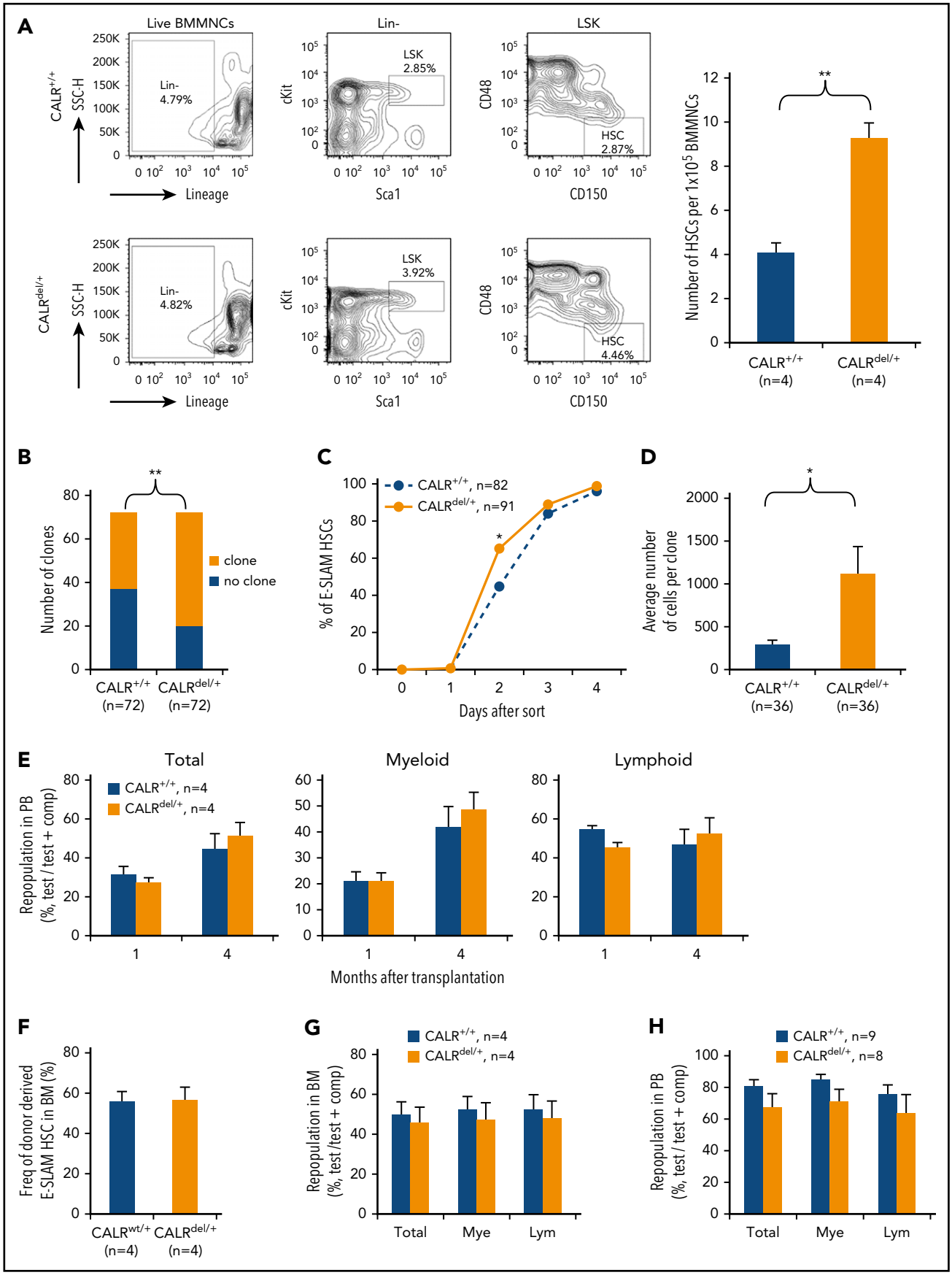

Figure 4.

demonstrated that CALR$^{fl/+}$ mice expressed levels of CALR comparable with that expressed by CALR$^{+/+}$ mice (supplemental Figure 1D).

CALR$^{del/+}$ mice develop a myeloproliferative phenotype resembling human ET

CALR$^{fl/+}$ mice were crossed with Mx1Cre transgenic mice,[21] and expression of Cre recombinase was induced with polyinosinic: polycytidylic acid (poly I:C) injection 6 to 8 weeks after birth. Mice carrying the recombined allele with mutant CALR expression were denoted CALR$^{del/+}$. Without poly I:C treatment, recombination did not occur at detectable levels, and blood counts were normal in Mx1Cre^{+} CALR$^{fl/+}$ mice (supplemental Figure 2A-B). By 4 weeks after poly I:C, genomic PCR showed recombination in more than 80% of nucleated blood cells (supplemental Figure 2C). Mutant CALR RNA expression was confirmed by RT-PCR in BM cells (supplemental Figure 2D). In hematopoietic stem and progenitor cells, transcript levels of mutant CALR were 65% to 72% (mean, 68%) of transcript levels from the WT allele as analyzed by fragment analysis (supplemental Figure 2E). A reduction in the level of mutant transcripts was also seen by using several different expression constructs (supplemental Figure 2F) and in a previously reported transgenic model,[18] indicating that lower levels of mutant CALR transcripts are not specific to the targeting construct used to generate our knockin mice and may instead reflect altered stability associated with the novel 3′ sequence. Levels of the mutant protein in CALR$^{del/del}$ mice were much lower than levels of WT protein in control cells (supplemental Figure 2G), an observation consistent with the previous demonstration that the mutant protein is unstable,[22,23] and also consistent with the results from a retroviral transplantation model.[17]

CALR$^{del/+}$ mice developed a striking thrombocytosis compared with WT littermate controls. White blood cell counts were mildly elevated in some but not all cohorts, and red blood cell parameters were not affected (Figure 2A). No difference in survival was observed in cohorts maintained for up to 8 months (supplemental Figure 3A). We also crossed CALR$^{fl/+}$ mice with VavCre transgenic mice.[24] Similar to results with Mx1Cre mice, VavCre mice had high rates of recombination in peripheral blood, and the mice developed thrombocytosis (supplemental Figure 3B-C).

In JAK2^{V617F} knockin mice, platelet reactivity to collagen-related peptide and thrombin agonists was increased.[25] We therefore studied platelet reactivity to several agonists including collagen-related peptide, thrombin, and adenosine 5′-diphosphate, but we observed no significant increase in response to any agonist using platelets from the CALR$^{del/+}$ mice (supplemental Figure 3D).

BM cellularity and spleen weight were not significantly affected in CALR$^{del/+}$ mice 3 to 4 months after injection of poly I:C (supplemental Figure 4A-B). Histologic analysis of BM from CALR$^{del/+}$ mice showed megakaryocytic hyperplasia, with megakaryocytes displaying large and hyperlobated nuclei and increased clustering (Figure 2B). Spleen architecture was not affected, although a degree of extramedullary hematopoiesis was observed in some cases, and there was no significant increase in reticulin staining in either BM or spleen at this time point (Figure 2B; supplemental Figure 4C). Compared with littermate controls, the BM of CALR$^{del/+}$ mice contained increased numbers of colony-forming unit megacaryocytes (Figure 2C) and megakaryocytes (Figure 2D) together with reduced numbers of CD71^{+}Ter119^{+} erythroblasts (Figure 2E). Numbers of myeloerythroid progenitor populations and more mature myeloid cells (Mac1^{+}Ly6g^{+}) in the BM were not significantly altered (supplemental Figure 4D). In the spleen, there was no significant alteration in the proportion of megakaryocytes, myeloid cells, or erythroblasts (supplemental Figure 4E). Taken together, these data demonstrate that CALR$^{del/+}$ mice displayed a marked thrombocytosis accompanied by increased megakaryopoiesis and compromised erythropoiesis in the BM.

Thrombocytosis in CALR$^{del/+}$ mice is transplantable

THPO levels were not increased in CALR$^{del/+}$ mice and were, if anything, reduced (although this did not reach statistical significance), suggesting that the thrombocytosis was not THPO driven and was likely to be cell intrinsic (Figure 3A). To confirm this inference, WT recipient mice were transplanted with BM cells from CALR$^{del/+}$ mice 2 months after poly I:C. At both 1 month and 4 months after transplantation, the level of chimerism was approximately 80% in peripheral blood mononuclear cells (PBMCs), myeloid cells (Ly6g^{+} and Mac1^{+}), and lymphoid cells (B220^{+} and CD3e^{+}) (Figure 3B; supplemental Figure 5A). Recipients of CALR$^{del/+}$ BM developed marked thrombocytosis, with platelet numbers similar to those in donor mice by 4 months after transplantation (Figure 3C). After secondary transplantations, recipients also developed thrombocytosis (Figure 3D), with donor chimerism at 4 months after transplantation being around 60% for PBMCs, myeloid cells, and lymphoid cells (Figure 3E; supplemental Figure 5B), indicating that thrombocytosis was still evident in the presence of 40% normal hematopoietic

Figure 4. Mutant CALR increases phenotypic HSCs with altered behavior in vitro but no self-renewal advantage in vivo. (A) CALR$^{del/+}$ mice show increased frequency of HSCs in the BM. Flow cytometry was performed on BM from mice at 3 to 4 months after poly I:C injection; HSC is defined as Lin^{-}Sca-1^{+}c-Kit^{+}CD150^{+}CD48^{-}. (B) CALR$^{del/+}$ E-SLAM HSCs have a significantly higher cloning efficiency than WT E-SLAM HSCs. Single E-SLAM cells were defined as successfully forming a clone if assayed to have more than 50 cells at day 7 as assessed by flow cytometry. Both CALR$^{+/+}$ and CALR$^{del/+}$ represent 72 individual E-SLAM HSCs from 3 independent experiments. *P* value was calculated from a χ^2 test. (C) E-SLAM HSCs from CALR$^{del/+}$ mice exhibit early cell division in a single-cell in vitro assay. Line graphs show that a significantly higher proportion of E-SLAM HSCs completed first division during the 4 days of single-cell in vitro analysis. Three independent experiments were performed. *P* value was calculated from a χ^2 test. (D) E-SLAM HSCs from CALR$^{del/+}$ mice form larger clones in vitro. After 7 days in culture, E-SLAM clones (irrespective of size) were analyzed by using flow cytometry, and the average number of cells per clone was measured. (E) BM cells from CALR$^{del/+}$ mice show similar repopulating capacity in peripheral blood (PB) of primary competitive transplants. Donor repopulation was assessed by using flow cytometry of nucleated peripheral blood with antibodies for CD45.1 and CD45.2 to distinguish donor origin, Ly6g and Mac1 for myeloid lineages, and B220 and CD3e for lymphoid lineages. Competitive repopulating ability is presented as the percentage of repopulated cells derived from test donor cells among the total number of donor-derived cells (ie, test/[test + competitor (comp)]). Bar graphs that show BM cells from CALR$^{del/+}$ mice exhibit comparable repopulating capacity to both myeloid and lymphoid cells in peripheral blood. (F) CALR$^{del/+}$ BM primary recipients show similar frequency of donor-derived E-SLAM HSCs compared with the control recipient mice. Flow cytometry was performed using antibodies for CD45.1 and CD45.2 together with antibodies for E-SLAM HSC markers. (G) BM cells from CALR$^{del/+}$ mice show similar repopulating capacity in BM of primary competitive transplants. Primary recipients were culled 4 months after transplantation and flow cytometry was performed as above to assess donor competitive repopulating ability in the BM. Bar graphs showing BM cells from CALR$^{del/+}$ mice exhibit comparable repopulating capacity to both myeloid (Mye) and lymphoid (Lym) lineages in the BM of the primary recipients. (H) BM cells from CALR$^{del/+}$ mice show similar repopulating capacity in secondary competitive transplants. Donor repopulation was assessed by using flow cytometry of peripheral blood as in panel E. Bar graphs showing comparable repopulating capacity to multiple lineages in peripheral blood in the secondary competitive transplantation recipients. Data are shown as mean ± SEM. $^{*}P < .05$; $^{**}P < .01$. SSC-H, side scatter.

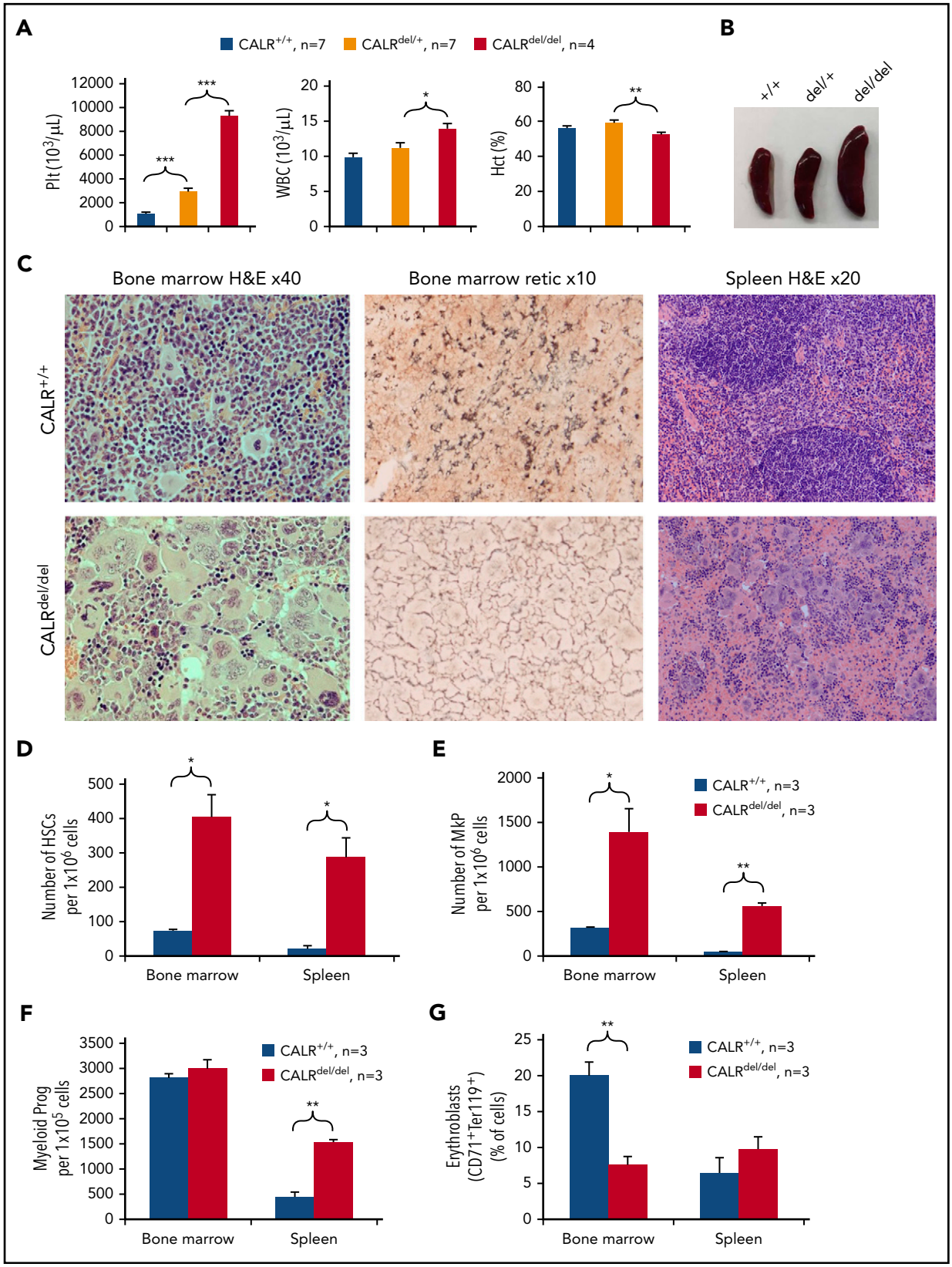

Figure 5. CALR$^{del/del}$ mice develop an extreme myeloproliferative disease with MF. (A) CALR$^{del/del}$ mice develop marked thrombocytosis. Bar graphs showing significantly increased platelets, elevated WBC counts, and reduced hematocrit (Hct) in CALR$^{del/del}$ mice at 3 to 4 months after poly I:C. The CALR$^{del/del}$ mice were CALR$^{fl/fl}$ Mx1Cre^{+}, the CALR$^{del/+}$ mice were CALR$^{fl/+}$ Mx1Cre^{+}, and the control mice (CALR$^{wt/+}$) were CALR$^{fl/+}$ Mx1Cre^{-} or CALR$^{+/+}$ Mx1Cre^{+}. (B) CALR$^{del/del}$ mice show splenomegaly. (C) CALR$^{del/del}$ mice show striking megakaryocytic hyperplasia. Tissues from mice at 7 to 8 months after poly C:I were taken for histologic analysis. (Left panel) H&E staining of BM showing almost complete effacement of normal hematopoiesis by megakaryocytes and displaying nuclear atypia in CALR$^{del/del}$ mice. (Middle panel) Silver staining for reticulin showing BM fibrosis in CALR$^{del/del}$ mice. (Right panel) H&E staining of spleen showing destruction of splenic architecture in CALR$^{del/del}$ mice. (D) CALR$^{del/del}$ mice show markedly increased frequencies of HSCs. Flow cytometry was performed

cells. These data demonstrate that the thrombocytosis in CALR$^{del/+}$ mice is transplantable and reflects a BM-cell intrinsic mechanism.

Mutant CALR is associated with increased proliferation of single HSCs in vitro but no self-renewal advantage in vivo

The BM of CALR$^{del/+}$ mice contained increased numbers of HSCs, both Lin$^-$Sca1$^+$cKit$^+$CD150$^+$CD48$^-$ HSCs (Figure 4A) and E-SLAM HSCs (CD45$^+$EPCR$^+$CD150$^+$CD48$^-$; supplemental Figure 6A). To examine the effect of mutant CALR on the behavior of HSCs, we studied the survival and cell division kinetics of single HSCs together with their ability to proliferate and differentiate.[19,20] Compared with WT controls, the proportion of single CALR$^{del/+}$ HSCs that gave rise to clones of more than 50 cells after 7 days in culture was significantly higher (Figure 4B). Single HSCs from CALR$^{del/+}$ mice showed significantly earlier cell division compared with those from littermate controls (Figure 4C) and formed larger clones after 7 days in culture (Figure 4D; supplemental Figure 6B). Although clones from CALR$^{del/+}$ HSCs were larger, flow cytometric analysis showed that they contained unaltered percentages of LSK, lineage-positive, Mac1$^+$, CD41$^+$, and CD71$^+$ cells (supplemental Figure 6C-E).

To investigate the functional consequences of mutant CALR on HSCs, competitive BM transplantation was performed by using cells from mice at 2 months after poly I:C. BM cells from CALR$^{del/+}$ or littermate control mice (both CD45.2) were mixed with equal numbers of CD45.1/45.2 F_1 competitor BM cells and transplanted into irradiated C57BL/6 recipients (CD45.1). The contribution of CALR$^{del/+}$ cells to recipient PBMCs, myeloid cells (Ly6g$^+$ and Mac1$^+$) and lymphoid cells (B220$^+$ and CD3e$^+$) was similar to that in littermate controls at 1 and 4 months after transplantation (Figure 4E). Recipients of CALR$^{del/+}$ BM did not develop thrombocytosis (supplemental Figure 6F), probably because donor chimerism was usually <50% in this setting. Analysis of the recipient BM 4 months after transplantation revealed a similar picture. Compared with control cells, CALR$^{del/+}$ cells showed no increase in their contribution to E-SLAM HSCs (Figure 4F) or myeloid and lymphoid lineages (Figure 4G). Secondary transplantations were performed, and at 4 months after transplantation, CALR$^{del/+}$ cells again showed no significant repopulation advantage (Figure 4H). Together, these data show that CALR$^{del/+}$ BM contains more phenotypically defined HSCs, and these cells exhibited increased proliferation in vitro, but the long-term in vivo repopulating activity of CALR$^{del/+}$ BM was normal.

Homozygosity for CALR mutation (CALR$^{del/del}$) results in severe thrombocytosis and development of MF

To assess the pathological consequences of homozygous expression of mutant CALR, CALR$^{fl/+}$ mice on an Mx1Cre background were crossed with each other to generate CALR$^{fl/fl}$ mice. Upon Cre recombination, mice with homozygous expression of mutant CALR (denoted as CALR$^{del/del}$) developed extreme thrombocytosis with platelet counts around 9000×10^9/L by 3 to 4 months after poly I:C (Figure 5A). This was accompanied by a modest but significant increase in white blood cell numbers and reduced hematocrit (Figure 5A). By 6 to 8 months after poly I:C, CALR$^{del/del}$ mice showed splenomegaly (Figure 5B; supplemental Figure 7A) and reduced BM cellularity (supplemental Figure 7B). Macroscopically, BM samples from the CALR$^{del/del}$ mice were paler and their spleen cell samples were redder in color compared with those of the littermate controls (supplemental Figure 7C). Histologic analysis of BM showed almost complete effacement of normal hematopoiesis by megakaryocytes that displayed nuclear atypia and were accompanied by increased levels of reticulin (Figure 5C; supplemental Figure 7D). Hematoxylin and eosin staining of sections of the spleen showed destruction of normal splenic architecture with markedly increased numbers of atypical megakaryocytes without increased levels of reticulin (Figure 5C; supplemental Figure 7E).

Flow cytometric analysis demonstrated that CALR$^{del/del}$ BM harbored substantially increased numbers of HSCs, both Lin$^-$Sca1$^+$cKit$^+$CD150$^+$CD48$^-$ HSCs (Figure 5D) and E-SLAM HSCs (supplemental Figure 7F). Marked increases in the proportion of MkPs (Lin$^-$Sca1$^-$cKit$^+$CD150$^+$CD41$^+$) were noted in both BM and spleen (Figure 5E). Myeloid progenitors (Lin$^-$Sca1$^-$cKit$^+$), pre–granulocyte-macrophage progenitors (preGM, Lin$^-$Sca1$^-$cKit$^+$CD41$^-$CD16/32$^-$CD105$^-$CD150$^-$), and granulocyte-macrophage progenitors (GMP, Lin$^-$Sca1$^-$cKit$^+$CD41$^-$CD16/32$^+$CD150$^-$) were expanded in CALR$^{del/del}$ mice (Figure 5F; supplemental Figure 7G), and erythroblasts (CD71$^+$Ter119$^+$) were reduced in BM, but pre-CFU–erythroid progenitors (preCFU-E, Lin$^-$Sca1$^-$cKit$^+$CD41$^-$CD16/32$^-$CD105$^+$CD150$^+$) were increased in the spleen (Figure 5G; supplemental Figure 7G). Taken together, these data demonstrate that homozygosity for mutant CALR produces a dramatic phenotype with extreme thrombocytosis and a marked increase in megakaryopoiesis, MF, and HSC expansion.

Noncompetitive BM transplantations were performed to determine whether this extreme thrombocytosis is transplantable. WT recipient mice were transplanted with BM cells from CALR$^{del/del}$ mice. At 4 months after transplantation, the level of chimerism was ~70% in PBMCs, myeloid cells (Ly6g$^+$ and Mac1$^+$), and lymphoid cells (B220$^+$ and CD3e$^+$) (Figure 6A). Recipients of CALR$^{del/del}$ BM developed a similar degree of thrombocytosis, with platelet numbers similar to those in the CALR$^{del/del}$ donor mice by 5 months posttransplantation as well as leukocytosis (Figure 6A). These data demonstrate that the extreme thrombocytosis in CALR$^{del/del}$ mice is transplantable. Competitive BM transplantation was performed to investigate the functional consequences of mutant CALR homozygosity on HSCs. BM cells from CALR$^{del/del}$ or littermate control mice (both CD45.2) were mixed with equal numbers of CD45.1/CD45.2 F_1 competitor BM cells and transplanted into irradiated Kit$^{W41/W41}$ C57BL/6 recipients (CD45.1). The contribution of CALR$^{del/del}$ cells to recipient peripheral blood, myeloid cells (Ly6g$^+$ and Mac1$^+$), and lymphoid cells (B220$^+$ and CD3e$^+$) was analyzed by flow cytometry and was similar to that in littermate controls (Figure 6B). At 4 months posttransplantation, secondary transplantations were performed, and analysis showed that

Figure 5 (continued) and HSCs were defined as Lin$^-$Sca1$^+$cKit$^+$CD150$^+$CD48$^-$. (E) CALR$^{del/del}$ mice show markedly increased frequencies of megakaryocytic progenitors (MkPs) (Lin$^-$Sca1$^-$cKit$^+$CD150$^+$CD41$^+$). (F) CALR$^{del/del}$ mice show markedly increased frequencies of myeloid progenitors (Prog) in spleen. Flow cytometry was performed, and myeloid progenitors were defined as the Lin$^-$Sca1$^-$cKit$^+$ population. (G) CALR$^{del/del}$ mice show significantly reduced numbers of erythroblasts. Flow cytometry was performed and erythroblasts were defined as CD71$^+$Ter119$^+$. Data are shown as mean ± SEM. *$P < .05$; **$P < .01$; ***$P < .001$.

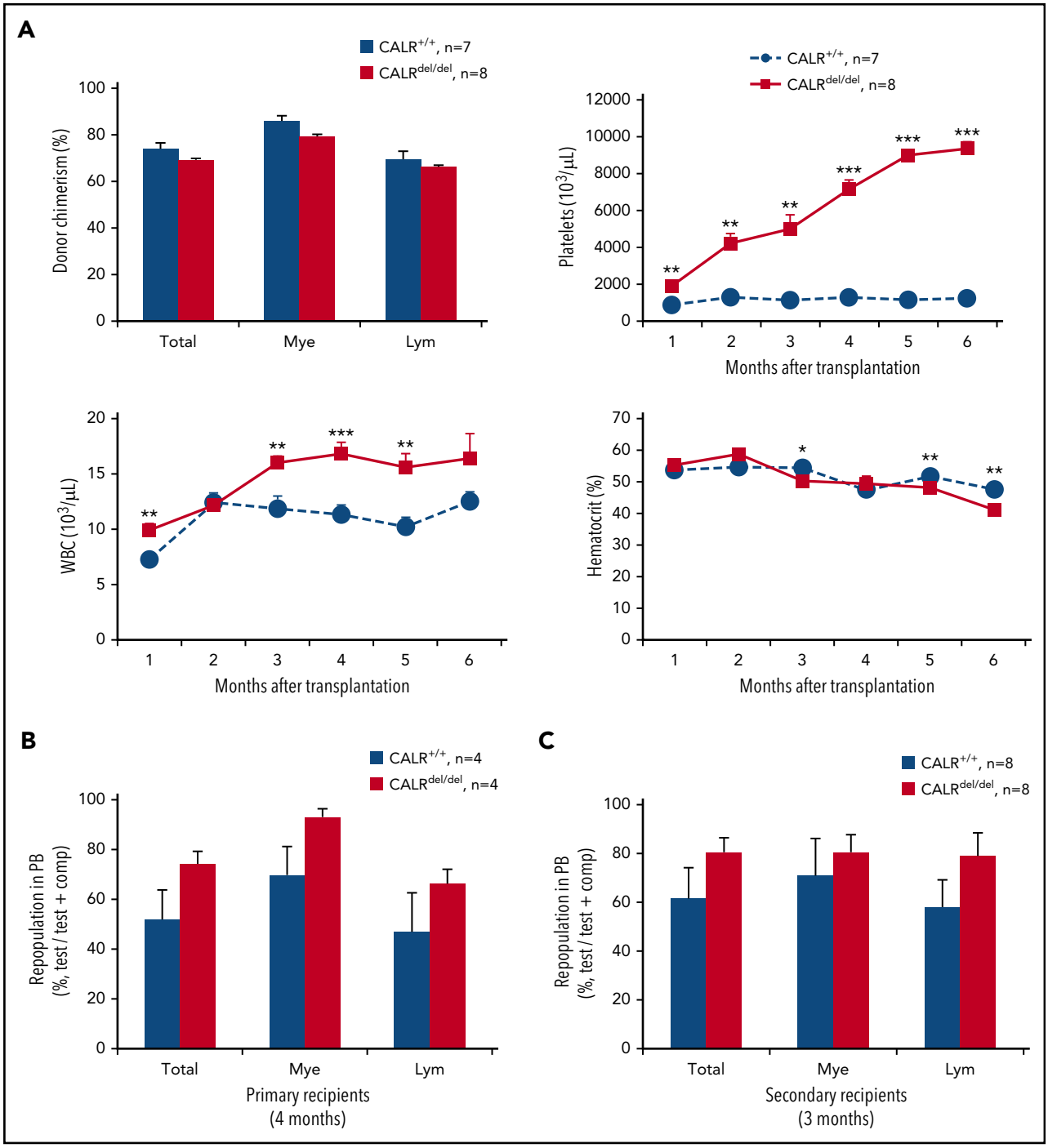

Figure 6. Mutant CALR homozygosity results in a transplantable extreme thrombocytosis but does not confer competitive repopulating advantage in serial transplants. (A) Donor chimerism is comparable in the primary noncompetitive BM transplants. BM cells from CALR$^{del/del}$ or control mice at 7 to 8 months after poly I:C (2×10^6 per recipient) were transplanted into irradiated (1×400 cGy) Kit$^{W41/W41}$ C57BL/6 recipients (CD45.1). Bar graphs show donor chimerism in peripheral blood, which was analyzed by using flow cytometry with CD45.1 and CD45.2 antibodies and is derived as the percentage of CD45.2$^+$ cells in whole nucleated blood. Time course of blood counts is shown, and significantly increased platelet counts were seen in the recipients of CALR$^{del/del}$ BM. (B) Bone marrow cells from CALR$^{del/del}$ mice show similar repopulating capacity in peripheral blood of primary competitive transplants. Donor repopulation was assessed by using flow cytometry as detailed in Figure 4E. (C) Bone marrow cells from CALR$^{del/del}$ mice show similar repopulating capacity in secondary competitive transplants. Donor repopulation was assessed by using flow cytometry of peripheral blood as in Figure 4E; bar graphs show comparable repopulating capacity to multiple lineages in peripheral blood in the secondary competitive transplantation recipients. Data are shown as mean ± SEM. *$P < .05$; **$P < .01$; ***$P < .001$.

CALR$^{del/del}$ cells exhibited similar competitive repopulating capacity in the secondary recipients (Figure 6C). Together, these data demonstrate that CALR$^{del/del}$ BM contains strikingly expanded phenotypically defined HSCs, but the long-term in vivo repopulating activity of CALR$^{del/del}$ BM is comparable to that in the WT controls.

Discussion

In this article, we describe a knockin mouse model of the most common CALR mutation, an approach that allowed us to explore the consequences of mutant CALR without the confounding

effects of additional mutations that are present in samples from MPN patients. The targeting strategy was chosen to result in expression of a murine CALR protein in which the WT C terminus is replaced by the mutant human C terminus found in MPN patients. After Cre-mediated recombination, the mutant transcript was expressed under the control of the full complement of endogenous CALR regulatory elements.

Heterozygous CALR$^{del/+}$ mice developed an ET-like phenotype with marked thrombocytosis, increased megakaryopoiesis, and abnormal BM megakaryocyte morphology. Hemoglobin and red cell levels were normal, and there was no increased reticulin staining in the BM. The results contrast with the phenotype of JAK2^{V617F} knockin mice in which platelet, hemoglobin, and leukocyte levels were elevated, and the BM contained increased erythroid, myeloid, and megakaryocytic progenitors.[26-29] Moreover, these differing phenotypes are consistent with what is observed in JAK2-mutant compared with CALR-mutant MPN patients. The isolated thrombocytosis seen in CALR$^{del/+}$ mice resembles that seen in CALR-mutant ET patients and, compared with JAK2-mutant ET patients, those carrying a CALR mutation have higher platelet levels with lower levels of hemoglobin and white blood cells.[30-33] Furthermore, the effect of mutant CALR on platelet reactivity was different from that previously observed with JAK2-mutant cells.[25] Although the former showed normal responses to platelet agonists, JAK2-mutant platelets were hyperreactive. These results are in keeping with the increased thrombosis rate observed in patients bearing JAK2 mutations.[32]

Homozygosity for CALR mutations has been observed in patients with ET,[13,33,34] but its pathogenetic consequences are unclear. Our results demonstrate that homozygosity for mutant CALR causes extreme thrombocytosis associated with increased white cell counts, reduced hemoglobin levels, splenomegaly, and increased levels of BM reticulin, a constellation of features that resembles myelofibrotic transformation of ET. This phenotype contrasts with that seen in mice homozygous for JAK2^{V617F}, which shows extreme elevation of hemoglobin levels and a decrease in platelet counts relative to those in mice heterozygous for JAK2^{V617F}.[35] Together, our data demonstrate clear differences in the consequences of CALR and JAK2 mutations, and that these differences are more pronounced in the homozygous setting.

Our results are in accord with observations made when using retroviral transplantations or transgenic mice that express the human mutant CALR.[14,17,18] Both approaches resulted in thrombocytosis and megakaryocytic hyperplasia, but MF was seen only in mice harboring retroviral constructs,[17] perhaps reflecting varying levels of expression achieved by these different approaches. This concept is consistent with our finding of MF in CALR$^{del/del}$ but not in CALR$^{del/+}$ mice.

Our results shed light on the role of mutant CALR within the HSC compartment. BM transplant studies demonstrated that the ET-like phenotype seen in CALR$^{del/+}$ mice could be propagated in both primary and secondary recipients. These results demonstrate that CALR-mutant long-term repopulating HSCs are able to give rise to features of ET even in secondary recipients in which chimerism levels were reduced to 60%. These observations are in accord with studies of patients with CALR-mutant ET, which showed that the CALR mutation is present in highly purified HSCs.[6] Moreover, analyses of individual hematopoietic colonies showed that the CALR mutation was present in the first mutant phylogenetic node in all 5 patients studied, indicating that it was likely to be an initiating mutation in these patients.[6]

However, our data show that mutant CALR does not confer a competitive HSC advantage in serial transplantations in either heterozygous or homozygous settings. This result is consistent with a report regarding a transgenic mouse model, which concluded that HSCs expressing mutant CALR exhibited normal self-renewal.[18] In a retroviral transplantation model, phenotypic green fluorescent protein–positive (GFP$^+$) LSK and GFP$^+$ SLAM LSK cells expanded over time in primary recipient mice.[17] However, secondary transplantations were not performed and therefore the impact on long-term HSC function remains unclear. Both transgenic and retroviral approaches are known to result in dysregulated expression, in terms of both transcript levels and pattern of expression, which may contribute to the distinct phenotypes.

It is interesting that our knockin mutant CALR mice (and 3 independent mutant JAK2 knockin mice[20,26,36,37]) all showed no HSC advantage in serial transplantation studies, despite mutant CALR (or mutant JAK2) being found as a sole driver mutation in a substantial proportion of MPN patients. There are several potential explanations (not mutually exclusive) for this apparent conundrum. First, genetic background may cooperate with mutant CALR. There is mounting evidence that genetic background influences HSC function in mice[38,39] and also the development of both MPNs[40-42] and clonal hematopoiesis.[43] Second, unidentified somatic driver mutations may cooperate with mutant CALR. It seems unlikely that many additional coding mutations remain to be discovered, but there is much less known about the role of somatic noncoding mutations that affect regulatory elements in tumors.[44-46] Third, age-related changes affecting the microenvironment (eg, niche or inflammatory signaling) may explain the association of MPNs with increasing age.[47-49] And fourth, lineage tracing studies suggest that steady-state hematopoiesis is supported by long-lived progenitors that may not read out in transplantation assays.[50,51]

Levels of the mutant protein were much lower than levels of WT protein, consistent with previous findings that the mutant protein is unstable[22,52] and less abundant compared with WT controls in a retroviral expression model.[17] We also noted that, in hematopoietic stem and progenitor cells from heterozygous knockin mice, mutant transcripts were expressed at lower levels (mean, 68%) relative to WT transcripts. We considered the possibility that this might reflect a technical problem with our construct and explain the lack of a clonal advantage. Although our data do not formally exclude this scenario, we believe this is highly unlikely for multiple reasons. First, the knockin construct gives rise to strong HSC, progenitor, megakaryocytic, and platelet phenotypes. HSC, progenitor cell, and platelet numbers are similar to or higher than those seen in the retroviral or transgenic mouse models.[14,17,18] Thus, our knockin construct clearly has functional consequences in multiple cell types and stages of differentiation. Second, the lack of an HSC clonal advantage is consistent with results obtained from the transgenic CALR model in which similar serial competitive transplantations were performed (see Figure 4C in Shide et al[18]). Third, in homozygous mice, which have double the dose of the mutant allele, we still see no clonal advantage in secondary transplantation recipients. This is inconsistent with the concept that a 32% decrease in mutant transcript levels is responsible for the lack of an HSC repopulation advantage. Fourth,

our results demonstrate that several mutant CALR expression constructs (which are completely different from our knockin construct [supplemental Figure 2F]) also give rise to lower transcript levels compared with WT controls. In addition, the transcript levels of mutant CALR in the transgenic model are reported to be 64% of those of WT levels (see Figure 3B in Shide et al[18]). Together, these data indicate that lower levels of mutant CALR transcript are not specific to the targeting construct for our knockin mice and may represent altered stability associated with the novel 3′ sequence in mice. It remains to be seen whether lower mutant CALR messenger RNA levels are also present in patient samples.

It is informative to compare the consequences of CALR and JAK2 mutations on HSCs. CALR$^{del/+}$ mice displayed an increased number of phenotypic HSCs, but whole BM serial transplantation experiments showed no functional alteration in competitive repopulation ability. Across several reported heterozygous JAK2^{V617F} knockin mouse models, phenotypic HSC frequency was variable, with some models having increased HSC numbers and others reporting a reduction.[20,23,37,53] Nevertheless, when secondary transplantations were performed, none of these models had a competitive self-renewal advantage compared with WT cells and, if anything, there was a functional decline in repopulating ability for JAK2$^{V617F/+}$ cells in secondary recipients.[20,26,36,37] In vitro, single E-SLAM HSCs from CALR$^{del/+}$ mice entered cell division earlier and produced substantially larger clones (threefold increase in size) but did not display aberrant differentiation characteristics compared with their WT counterparts. In contrast, single HSCs from heterozygous JAK2 mice did not show changes in early cell divisional kinetics but did give rise to larger, more differentiated clones. Notably, these clones contained increased lineage-positive cells and reduced stem/progenitor (LSK) cells.[20] Thus, although both mutant JAK2 and CALR can drive a myeloproliferative phenotype, their HSCs have distinct features both in vivo and in vitro, suggesting differences in downstream signaling pathways and in mechanisms of clonal expansion.

Taken together, our results support the concept that ET consists of biologically distinct entities associated with different mutations. It seems likely that it will become increasingly important to subclassify MPNs on the basis of their underlying causal mutations instead of relying on their phenotypic consequences (eg, levels of hematocrit or megakaryocytic morphology). Recent results suggest that the different consequences of CALR and JAK2 mutations reflect, at least in part, differential interaction of mutant CALR and JAK2 with the homodimeric cytokine receptor EPOR, THPO receptor, and GCSFR, with mutant CALR preferentially binding to and activating the THPO receptor.[14,15] Our mouse model provides a powerful tool to further dissect the mechanisms by which mutant CALR contributes to MPN pathogenesis.

Acknowledgments

The authors thank Wanfeng Zhao, at The Human Research Tissue Bank (supported by the National Institute for Health Research Cambridge Biomedical Research Centre) for processing histologic sections and staining, and Reiner Schulte, Chiara Cossetti, and Gabriela Grondys-Kotarba for flow cytometry assistance at Cambridge Institute for Medical Research.

This work (Green laboratory) was supported by Bloodwise, Cancer Research UK, Wellcome Trust, the National Institute for Health Research Cambridge Biomedical Research Centre, the Cambridge Experimental Cancer Medicine Centre, and the Leukemia & Lymphoma Society of America. Work in the Kent laboratory was supported by grants from Bloodwise (15008), the European Hematology Association, and the European Research Council (ERC-2016-StG-715371). Additional support was provided by a European Molecular Biology Laboratory Long-Term Fellowship No. ALTF 1132-2015 (D.P.), by Bloodwise and the Kay Kendall Leukaemia Fund (J.G.), and by the Kay Kendall Leukaemia Fund (C.G.-A.).

Authorship

Contribution: J.L. designed and performed experiments and analyzed the data with input from D.P. on lineage and single HSC analysis, H.J.P. on flow cytometry analysis, C.G.-A. on megakaryocyte colony assays, J.G. on histology, O.M.D. on generating the model, T.K. on fragment analysis, and C.B. on platelet reactivity analysis; T.L.H., D.C.P., R.S., M.W., and J.A. helped with generation and phenotypic analysis of the mouse cohorts; C.G. collaborated on platelet analysis; G.S.V. collaborated in the generation of the knockin model; D.G.K. collaborated on HSC analysis; J.L. and A.R.G. wrote the paper with input from D.P., S.L., and D.G.K.; and A.R.G. directed the research.

Conflict-of-interest disclosure: The authors declare no competing financial interests.

Correspondence: Anthony R. Green, University of Cambridge, Cambridge Institute for Medical Research, Hills Rd, Cambridge CB2 0XY, United Kingdom; e-mail: arg1000@cam.ac.uk.

Footnotes

Submitted 12 September 2017; accepted 15 December 2017. Prepublished online as *Blood* First Edition paper, 27 December 2017; DOI 10.1182/blood-2017-09-806356.

*J.L. and D.P. contributed equally to this study.

The online version of this article contains a data supplement.

The publication costs of this article were defrayed in part by page charge payment. Therefore, and solely to indicate this fact, this article is hereby marked "advertisement" in accordance with 18 USC section 1734.

REFERENCES

1. Mead AJ, Mullally A. Myeloproliferative neoplasm stem cells. *Blood*. 2017;129(12):1607-1616.
2. Vainchenker W, Kralovics R. Genetic basis and molecular pathophysiology of classical myeloproliferative neoplasms. *Blood*. 2017;129(6):667-679.
3. Grinfeld J, Nangalia J, Green AR. Molecular determinants of pathogenesis and clinical phenotype in myeloproliferative neoplasms. *Haematologica*. 2017;102(1):7-17.
4. Campbell PJ, Green AR. The myeloproliferative disorders. *N Engl J Med*. 2006;355(23):2452-2466.
5. Beer PA, Erber WN, Campbell PJ, Green AR. How I treat essential thrombocythemia. *Blood*. 2011;117(5):1472-1482.
6. Nangalia J, Massie CE, Baxter EJ, et al. Somatic CALR mutations in myeloproliferative neoplasms with nonmutated JAK2. *N Engl J Med*. 2013;369(25):2391-2405.
7. James C, Ugo V, Le Couédic JP, et al. A unique clonal JAK2 mutation leading to constitutive signalling causes polycythaemia vera. *Nature*. 2005;434(7037):1144-1148.
8. Baxter EJ, Scott LM, Campbell PJ, et al; Cancer Genome Project. Acquired mutation of the tyrosine kinase JAK2 in human myeloproliferative disorders. *Lancet*. 2005;365(9464):1054-1061.
9. Kralovics R, Passamonti F, Buser AS, et al. A gain-of-function mutation in JAK2 in myeloproliferative disorders. *N Engl J Med*. 2005;352(17):1779-1790.

10. Levine RL, Wadleigh M, Cools J, et al. Activating mutation in the tyrosine kinase JAK2 in polycythemia vera, essential thrombocythemia, and myeloid metaplasia with myelofibrosis. *Cancer Cell*. 2005;7(4):387-397.

11. Scott LM, Tong W, Levine RL, et al. JAK2 exon 12 mutations in polycythemia vera and idiopathic erythrocytosis. *N Engl J Med*. 2007; 356(5):459-468.

12. Pikman Y, Lee BH, Mercher T, et al. MPLW515L is a novel somatic activating mutation in myelofibrosis with myeloid metaplasia. *PLoS Med*. 2006;3(7):e270.

13. Klampfl T, Gisslinger H, Harutyunyan AS, et al. Somatic mutations of calreticulin in myeloproliferative neoplasms. *N Engl J Med*. 2013; 369(25):2379-2390.

14. Elf S, Abdelfattah NS, Chen E, et al. Mutant calreticulin requires both its mutant C-terminus and the thrombopoietin receptor for oncogenic transformation. *Cancer Discov*. 2016;6(4): 368-381.

15. Chachoua I, Pecquet C, El-Khoury M, et al. Thrombopoietin receptor activation by myeloproliferative neoplasm associated calreticulin mutants. *Blood*. 2016;127(10):1325-1335.

16. Araki M, Yang Y, Masubuchi N, et al. Activation of the thrombopoietin receptor by mutant calreticulin in CALR-mutant myeloproliferative neoplasms. *Blood*. 2016;127(10): 1307-1316.

17. Marty C, Pecquet C, Nivarthi H, et al. Calreticulin mutants in mice induce an MPL-dependent thrombocytosis with frequent progression to myelofibrosis. *Blood*. 2016; 127(10):1317-1324.

18. Shide K, Kameda T, Yamaji T, et al. Calreticulin mutant mice develop essential thrombocythemia that is ameliorated by the JAK inhibitor ruxolitinib. *Leukemia*. 2017;31(5):1136-1144.

19. Kent DG, Dykstra BJ, Cheyne J, Ma E, Eaves CJ. Steel factor coordinately regulates the molecular signature and biologic function of hematopoietic stem cells. *Blood*. 2008;112(3): 560-567.

20. Kent DG, Li J, Tanna H, et al. Self-renewal of single mouse hematopoietic stem cells is reduced by JAK2V617F without compromising progenitor cell expansion. *PLoS Biol*. 2013; 11(6):e1001576.

21. Kühn R, Schwenk F, Aguet M, Rajewsky K. Inducible gene targeting in mice. *Science*. 1995;269(5229):1427-1429.

22. Han L, Schubert C, Köhler J, et al. Calreticulin-mutant proteins induce megakaryocytic signaling to transform hematopoietic cells and undergo accelerated degradation and Golgi-mediated secretion. *J Hematol Oncol*. 2016;9(1):45.

23. Yan D, Hutchison RE, Mohi G. Critical requirement for Stat5 in a mouse model of polycythemia vera. *Blood*. 2012;119(15): 3539-3549.

24. Stadtfeld M, Graf T. Assessing the role of hematopoietic plasticity for endothelial and hepatocyte development by non-invasive lineage tracing. *Development*. 2005;132(1): 203-213.

25. Hobbs CM, Manning H, Bennett C, et al. JAK2V617F leads to intrinsic changes in platelet formation and reactivity in a knock-in mouse model of essential thrombocythemia. *Blood*. 2013;122(23):3787-3797.

26. Li J, Spensberger D, Ahn JS, et al. JAK2 V617F impairs hematopoietic stem cell function in a conditional knock-in mouse model of JAK2 V617F-positive essential thrombocythemia. *Blood*. 2010;116(9):1528-1538.

27. Akada H, Yan D, Zou H, Fiering S, Hutchison RE, Mohi MG. Conditional expression of heterozygous or homozygous Jak2V617F from its endogenous promoter induces a polycythemia vera-like disease. *Blood*. 2010; 115(17):3589-3597.

28. Mullally A, Lane SW, Ball B, et al. Physiological Jak2V617F expression causes a lethal myeloproliferative neoplasm with differential effects on hematopoietic stem and progenitor cells. *Cancer Cell*. 2010;17(6):584-596.

29. Marty C, Lacout C, Martin A, et al. Myeloproliferative neoplasm induced by constitutive expression of JAK2V617F in knock-in mice. *Blood*. 2010;116(5):783-787.

30. Tefferi A, Guglielmelli P, Larson DR, et al. Long-term survival and blast transformation in molecularly annotated essential thrombocythemia, polycythemia vera, and myelofibrosis. *Blood*. 2014;124(16):2507-2513.

31. Tefferi A, Wassie EA, Lasho TL, et al. Calreticulin mutations and long-term survival in essential thrombocythemia. *Leukemia*. 2014;28(12):2300-2303.

32. Rotunno G, Mannarelli C, Guglielmelli P, et al; Associazione Italiana per la Ricerca sul Cancro Gruppo Italiano Malattie Mieloproliferative Investigators. Impact of calreticulin mutations on clinical and hematological phenotype and outcome in essential thrombocythemia. *Blood*. 2014;123(10):1552-1555.

33. Rumi E, Pietra D, Pascutto C, et al; Associazione Italiana per la Ricerca sul Cancro Gruppo Italiano Malattie Mieloproliferative Investigators. Clinical effect of driver mutations of JAK2, CALR, or MPL in primary myelofibrosis. *Blood*. 2014;124(7):1062-1069.

34. Theocharides AP, Lundberg P, Lakkaraju AK, et al. Homozygous calreticulin mutations in patients with myelofibrosis lead to acquired myeloperoxidase deficiency. *Blood*. 2016; 127(25):3253-3259.

35. Li J, Kent DG, Godfrey AL, et al. JAK2V617F homozygosity drives a phenotypic switch in myeloproliferative neoplasms, but is insufficient to sustain disease. *Blood*. 2014; 123(20):3139-3151.

36. Mullally A, Bruedigam C, Poveromo L, et al. Depletion of Jak2V617F myeloproliferative neoplasm-propagating stem cells by interferon-α in a murine model of polycythemia vera. *Blood*. 2013;121(18):3692-3702.

37. Hasan S, Lacout C, Marty C, et al. JAK2V617F expression in mice amplifies early hematopoietic cells and gives them a competitive advantage that is hampered by IFNα. *Blood*. 2013;122(8):1464-1477.

38. Zhou X, Crow AL, Hartiala J, et al. The genetic landscape of hematopoietic stem cell frequency in mice. *Stem Cell Reports*. 2015; 5(1):125-138.

39. de Haan G, Nijhof W, Van Zant G. Mouse strain-dependent changes in frequency and proliferation of hematopoietic stem cells during aging: correlation between lifespan and cycling activity. *Blood*. 1997;89(5): 1543-1550.

40. Landgren O, Goldin LR, Kristinsson SY, Helgadottir EA, Samuelsson J, Björkholm M. Increased risks of polycythemia vera, essential thrombocythemia, and myelofibrosis among 24,577 first-degree relatives of 11,039 patients with myeloproliferative neoplasms in Sweden. *Blood*. 2008;112(6):2199-2204.

41. Jones AV, Cross NC. Inherited predisposition to myeloproliferative neoplasms. *Ther Adv Hematol*. 2013;4(4):237-253.

42. Tapper W, Jones AV, Kralovics R, et al. Genetic variation at MECOM, TERT, JAK2 and HBS1L-MYB predisposes to myeloproliferative neoplasms. *Nat Commun*. 2015;6:6691.

43. Hinds DA, Barnholt KE, Mesa RA, et al. Germ line variants predispose to both JAK2 V617F clonal hematopoiesis and myeloproliferative neoplasms. *Blood*. 2016;128(8):1121-1128.

44. Mansour MR, Abraham BJ, Anders L, et al. Oncogene regulation. An oncogenic super-enhancer formed through somatic mutation of a noncoding intergenic element. *Science*. 2014;346(6215):1373-1377.

45. Horn S, Figl A, Rachakonda PS, et al. TERT promoter mutations in familial and sporadic melanoma. *Science*. 2013;339(6122):959-961.

46. Heidenreich B, Rachakonda PS, Hemminki K, Kumar R. TERT promoter mutations in cancer development. *Curr Opin Genet Dev*. 2014;24: 30-37.

47. Vassiliou GS. JAK2 V617F clonal disorders: fate or chance? *Blood*. 2016;128(8): 1032-1033.

48. Manshouri T, Estrov Z, Quintás-Cardama A, et al. Bone marrow stroma-secreted cytokines protect JAK2(V617F)-mutated cells from the effects of a JAK2 inhibitor. *Cancer Res*. 2011; 71(11):3831-3840.

49. Fleischman AG, Aichberger KJ, Luty SB, et al. TNFα facilitates clonal expansion of JAK2V617F positive cells in myeloproliferative neoplasms. *Blood*. 2011;118(24):6392-6398.

50. Sun J, Ramos A, Chapman B, et al. Clonal dynamics of native haematopoiesis. *Nature*. 2014;514(7522):322-327.

51. Busch K, Klapproth K, Barile M, et al. Fundamental properties of unperturbed haematopoiesis from stem cells in vivo. *Nature*. 2015;518(7540):542-546.

52. Kollmann K, Warsch W, Gonzalez-Arias C, et al. A novel signalling screen demonstrates that CALR mutations activate essential MAPK signalling and facilitate megakaryocyte differentiation. *Leukemia*. 2017;31(4):934-944.

53. Chen E, Schneider RK, Breyfogle LJ, et al. Distinct effects of concomitant Jak2V617F expression and Tet2 loss in mice promote disease progression in myeloproliferative neoplasms. *Blood*. 2015;125(2):327-335.